ISSN 3023-5669 Journal of Material Characterization and Applications, Vol. **3**, No. 3, pp 35-42 (2025)
www.matcharappjournal.com
https://doi.org/10.5281/zenodo.18110361

THE EFFECT OF Sm ADDITION ON THE MICROSTRUCTURAL AND HARDNESS PROPERTIES IN Al–Fe–Mn ALLOY

Ecem Ayşe ÇAKIR [a*]
Funda Gül KOÇ [b]
Fulya KAHRIMAN[c]

[a]**Kocaeli University, Faculty of Engineering, Department of Metallurgical and Materials Engineering, Kocaeli*
E-mail: *ecemcakir2001@gmail.com, ORCID ID: 0009-0000-5857-6158*

[b]*Kocaeli University, Faculty of Engineering, Department of Metallurgical and Materials Engineering, Kocaeli*
E-mail: *fundagulkoc@gmail.com, ORCID ID: 0000-0001-6517-1239*

[c]*Kocaeli University, Faculty of Engineering, Department of Metallurgical and Materials Engineering, Kocaeli*
E-mail: *fulya.kahriman@kocaeli.edu.tr, ORCID ID: 0000-0001-9609-0562*

Received 24 October 2025; revised 27 November 2025; accepted 22 December 2025

Abstract

Al–Fe–Mn alloys are widely preferred in packaging, automotive, and heat exchanger applications due to their high corrosion resistance, good formability, and thermal stability. The addition of rare earth elements to the aluminum matrix enhances the microstructure through mechanisms such as grain refinement, modification of intermetallic phases, and improved matrix stability, thereby increasing the mechanical and functional performance of the alloys. In this study, the effect of Sm addition on the microstructural properties of the Al–Fe–Mn alloy was investigated. For this purpose, alloys containing 0, 0.2, 0.4, and 0.6 wt.% Sm were produced by melting and casting, followed by homogenization heat treatment. After homogenization, the samples were prepared metallographically and characterized using optical microscopy and scanning electron microscopy (SEM) equipped with energy-dispersive X-ray spectroscopy (EDX). In order to determine the effect of Sm addition on the hardness of the alloy, comparative hardness measurements were carried out on the samples. The results revealed that increasing Sm content weakened the eutectic structure, significantly refined the grain size, and led to a more uniform distribution of Fe-based intermetallic phases. Furthermore, the formation of Sm–Fe intermetallic phases (Sm_2Fe, Sm_3Fe, Sm_5Fe) contributed to an increase in hardness values.

Keywords: Al–Fe–Mn Alloy, rare earth element, microstructural characterization, hardness

I. Introduction

Aluminum alloys are widely used in many fields ranging from automotive, aerospace, and space applications to packaging and the energy sector due to their low density, good formability, and high corrosion resistance [1]. The 8xxx series, which is based on the Al–Fe–Mn microstructure, stands out with its mechanical strength and thermal performance [2]. In the industrial sector, the Al–Fe–Mn alloy, also referred to as 8006M, is considered a reliable option for packaging materials and heat exchangers. Its excellent rolling properties, superior surface quality, and moderate mechanical strength make it suitable for applications in the food, pharmaceutical, and automotive industries [3]. During solidification, intermetallic compounds such as Al_3Mn, Al_3Fe, and $Al_3(Fe,Mn)$ play a crucial role in shaping the microstructure of this alloy. The casting parameters directly influence the geometry and distribution of these phases within the matrix [4–5].

Nowadays, the use of rare earth elements for microalloying in aluminum alloys has become an important approach for microstructural control and performance enhancement. Studies have shown that the addition of samarium leads to a significant reduction in the size of α-Al grains and in the eutectic configuration. This phenomenon is associated with a decrease in nucleation temperature and the suppression of Al_3Ni phase formation [6]. The addition of 1 wt.% samarium improves mechanical properties and wear resistance after casting and heat treatment, owing to its ability to strengthen the microstructure and contribute to phase modification [7]. Samarium reacts with iron in Al–Fe–Mn alloys to form intermetallic compounds such as $SmFe_2$, $SmFe_3$, and Al–Sm phases. X-ray diffraction (XRD) analyses confirm the presence of these phases. Reports indicate that $SmFe_7$ and Sm_2Fe_{17} phases become dominant with increasing iron content, whereas $SmFe_2$ and $SmFe_3$ phases are more frequently observed at lower iron concentrations [8]. These phases tend to accumulate in segregation regions and have a direct impact on microstructural evolution.

The existing literature reveals that only a limited number of studies have specifically investigated the effects of samarium addition on the 8006 alloy. Most research has focused on different alloy systems such as Al–Si, Al–Mg, and Al–Ni. However, the influence of samarium concentration on intermetallic phase evolution, phase transformation sequence, and microstructural changes in the 8006 alloy has not been comprehensively evaluated [9–10]. Experimental evidence suggests that $Al_6(Fe,Mn)$ phases produced under different solidification rates exhibit finer and more homogeneous intermetallic structures when samarium is added [11-13].

2. Materials and Methods

Within the scope of this study, the effect of Sm addition on the microstructural properties of the Al–Fe–Mn alloy was examined in detail; phase morphologies, grain structures, and orientation characteristics were determined using optical microscopy, SEM observations, and EDX analyses. In addition, comparative hardness measurements were performed to evaluate the influence of Sm on the hardness of the alloy. Alloys containing 0, 0.2, 0.4, and 0.6 wt.% Sm were melted in an induction furnace at 780 °C under controlled atmosphere conditions. The molten metal was poured into a metallic mold at 25 °C to obtain ingots with a thickness of approximately 5 mm. Following casting, the materials were subjected to homogenization treatment at 580 °C for eight hours. Samples for microstructural examinations were then prepared metallographically. During sample preparation, grinding was carried out sequentially with 60, 150, 220, 320, 600, 1000, and 2000 mesh abrasive papers, followed by polishing with 3 μm and 1 μm diamond suspensions. Etching was performed electrolytically at room temperature using a tetrafluoroboric acid–diethyl ether solution. Microstructural analyses were conducted using an Olympus BX41MLED optical microscope and a scanning electron microscope (SEM) equipped with an energy-dispersive X-ray spectroscopy (EDX) attachment. Hardness measurements were carried out with a Future Tech hardness tester under a load of 1 kg applied for 10 seconds, and five measurements were taken from each sample to obtain average hardness values.

3. Results and Discussion

Figure 1 presents the optical microscope images of Al–Fe–Mn alloys with different compositions. It is evident that Sm addition has a pronounced effect on the microstructure of the alloy. For the standard alloy (S0), coarse and irregular grain structures together with oriented intermetallic phases were observed as the main microstructural features. The alloy containing 0.2 wt.% Sm (S2) exhibited an increase in the density of intermetallic phases compared to the standard structure, a disruption of the eutectic configuration, and the formation of rod-like morphologies. In this case, the dendritic structure was not suppressed, leading to an increased tendency for crack formation and brittleness. For the alloy with 0.4 wt.% Sm (S4), the eutectic structure was further degraded, large intermetallic particles appeared, and the Fe content increased. At this composition, the structure remained heterogeneous, and the presence of brittle phases persisted. The alloy containing 0.6 wt.% Sm (S6), however, showed that Sm was incorporated more intensively into the phases, increasing their distinctiveness in the microstructure, while the dendritic structure was largely eliminated, resulting in the formation of a homogeneous grain structure. In this case, Sm addition provided structural refinement, created nucleation sites, and contributed to a more uniform distribution of secondary phases.

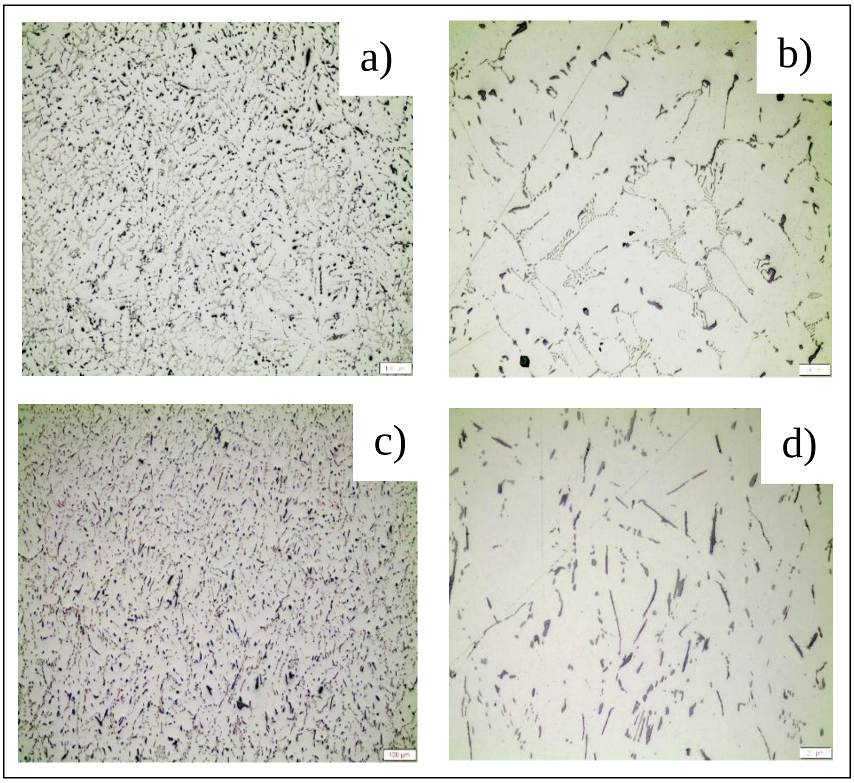

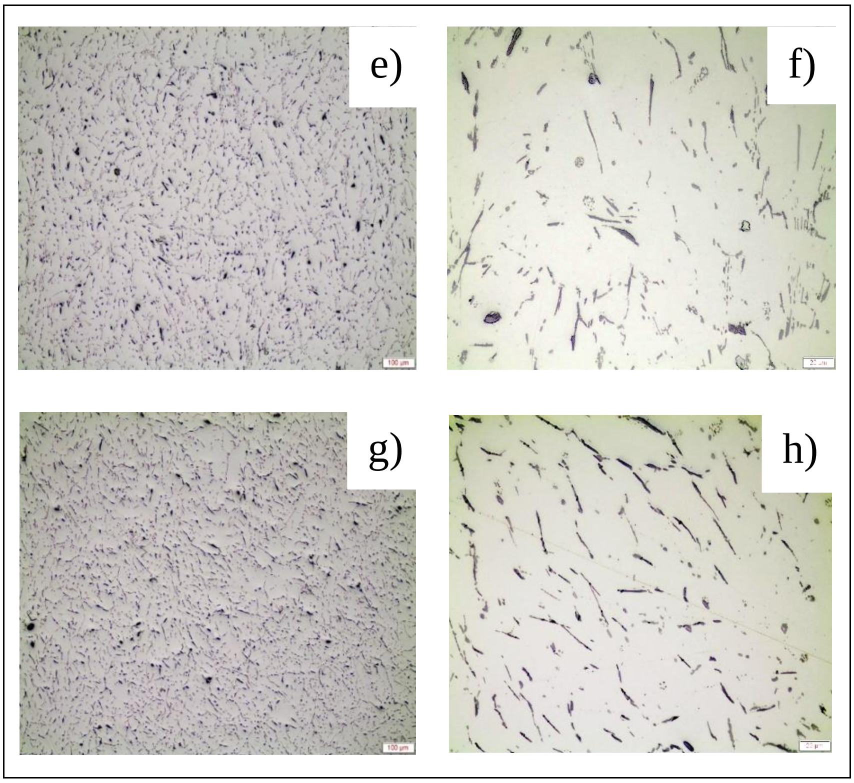

Figure 1. Optical microscope images of etched samples with different chemical compositions: a–b) standard alloy without Sm addition (S0), c–d) alloy with 0.2 wt.% Sm (S2), e–f) alloy with 0.4 wt.% Sm (S4), g–h) alloy with 0.6 wt.% Sm (S6).

Figure 2 shows the SEM images of Al–Fe–Mn alloys with standard composition and different amounts of Sm addition. In the homogenized standard sample (S0-HT), a dendritic solidification structure and contrasting intermetallic regions in the interdendritic areas were observed. In the sample containing 0.2 wt.% Sm (S2), a tendency toward refinement was initiated, and more compact intermetallic structures appeared. In the alloy with 0.4 wt.% Sm (S4), needle-like and rod-shaped β–Al_5FeSi and Al_3Fe phases, together with a network-like α–$Al_{15}(Fe,Mn)_3Si_2$ phase, became more pronounced; the rounding of the ends and the reduction in interface sharpness were notable. In the alloy containing 0.6 wt.% Sm (S6), Sm–Fe intermetallic phases (Sm_2Fe, Sm_3Fe, Sm_5Fe) developed in polygonal block-like morphologies, edge dissolution increased, and the continuity of the interdendritic network weakened. These findings indicate that as the Sm content increases, the refinement tendency is strengthened and microstructural homogeneity is significantly improved.

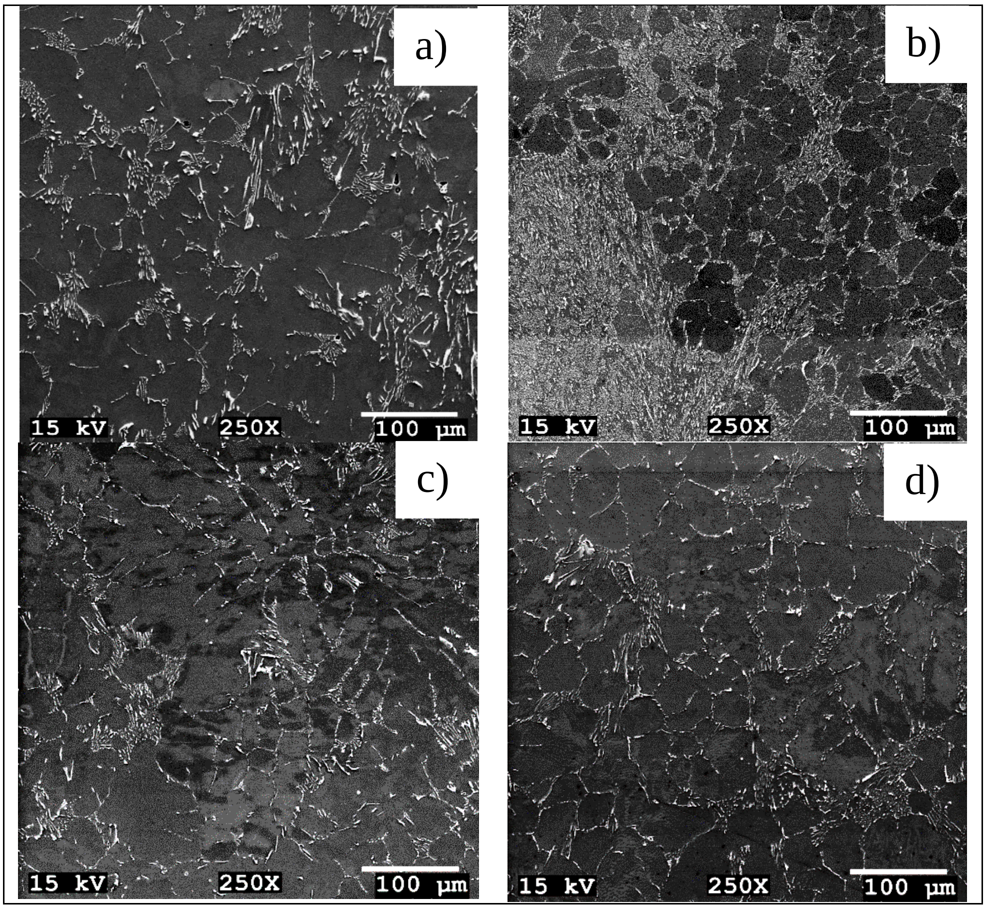

Figure 2. SEM images of etched samples with different chemical compositions: a) standard alloy without Sm addition (S0-HT); b) alloy with 0.2 wt.% Sm (S2); c) alloy with 0.4 wt.% Sm (S4); d) alloy with 0.6 wt.% Sm (S6).

Spot results of EDX analysis performed to determine the elemental compositions of phases observed in the microstructure of the Al–Fe–Mn alloy containing 0.4 wt.% Sm are given in Figure 3. In region 1, an Fe-rich intermetallic phase was identified with the following composition: Fe (9.27%), Mn (2.44%), Si (2.57%), and Sm (1.32%), in addition to Al. In region 2, the Al matrix was dominant (99.31%), while other elements remained at trace levels (Sm 0.31%, Fe 0.19%, Mn 0.17%, Si 0.01%). In region 3, the Al matrix was again dominant (99.02%), but the relative Sm content increased (0.55%). In region 4, the Al matrix was still dominant, with Mn and Fe signals detected at trace levels, and Sm present at low intensity. Overall, these results indicate that Sm tends to distribute at low levels within the matrix while showing an accumulation tendency in intermetallic regions, and that Fe-rich areas exhibit an intermetallic character composed of Al–Fe–Mn–Si phases.

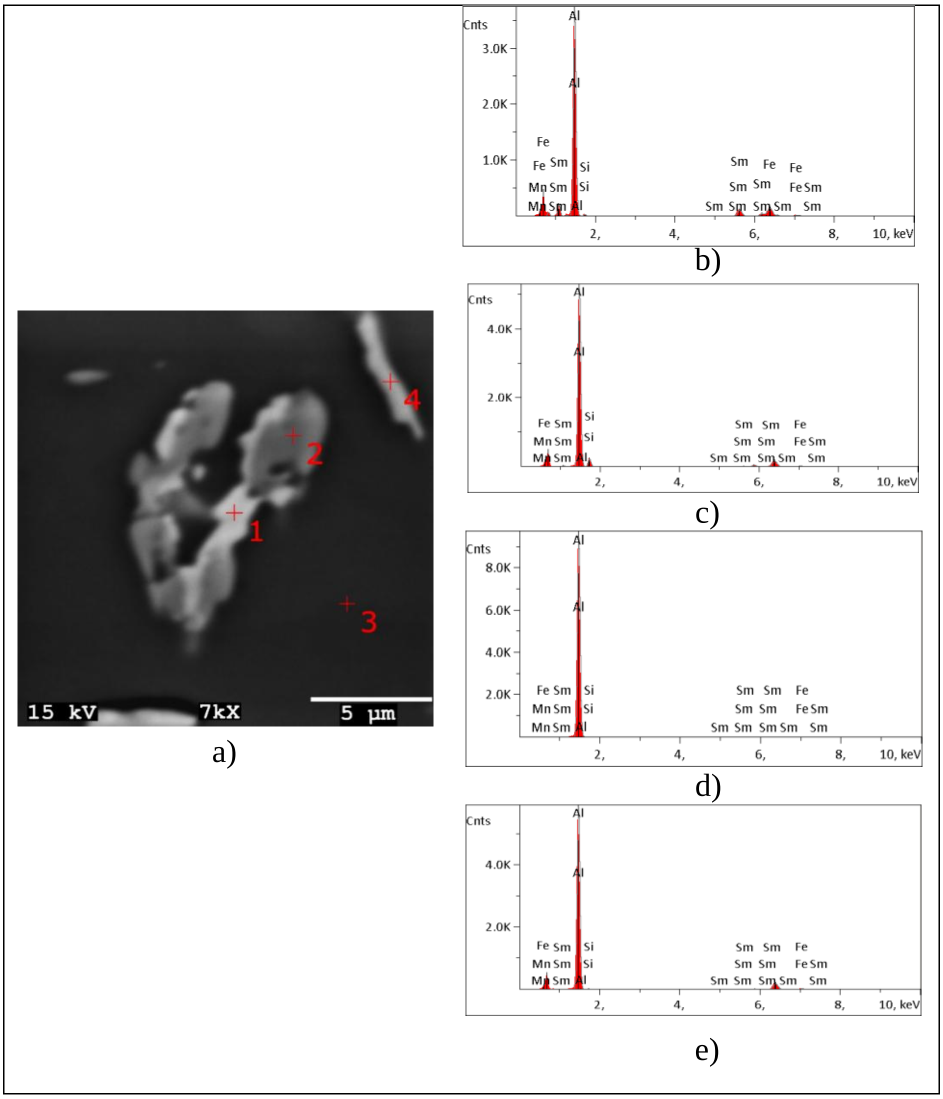

Figure 3. Al–Fe–Mn alloy with 0.4 wt.% Sm addition: a) SEM image, b) EDX analysis of region 1, c) EDX analysis of region 2, d) EDX analysis of region 3, e) EDX analysis of region 4.

Comparison of hardness values obtained as a result of Sm addition to Al–Fe–Mn alloys is givwn in Figure 4. The sample containing 0.2 wt.% Sm (S2) exhibited a hardness of approximately 36 HV1; this increase was associated with the formation of Sm_2Fe phases. In the sample with 0.4 wt.% Sm (S4), the hardness value increased to about 42 HV1, with the contribution of Sm_3Fe and Sm_5Fe phases becoming more pronounced. The sample containing 0.6 wt.% Sm (S6) showed a hardness of approximately 48 HV1; at this level, in addition to Sm–Fe intermetallic phases, the increase in Mg content also contributed to solid solution strengthening, thereby raising the overall hardness. However, due to the low coherency of Sm phases with the matrix and their relatively coarse particle sizes, the hardness improvement remained more limited compared to the Er series. Furthermore, the needle-like and network-shaped intermetallic phases observed in Sm-containing samples contributed to hardness enhancement. Nevertheless, the poor compatibility of Sm phases with the matrix and the relatively large particle sizes restricted the degree of hardness increase. The literature reports that Sm addition contributes to improvements in hardness and strength in Al-based alloys, but its effect is more limited compared to elements that form coherent precipitates.

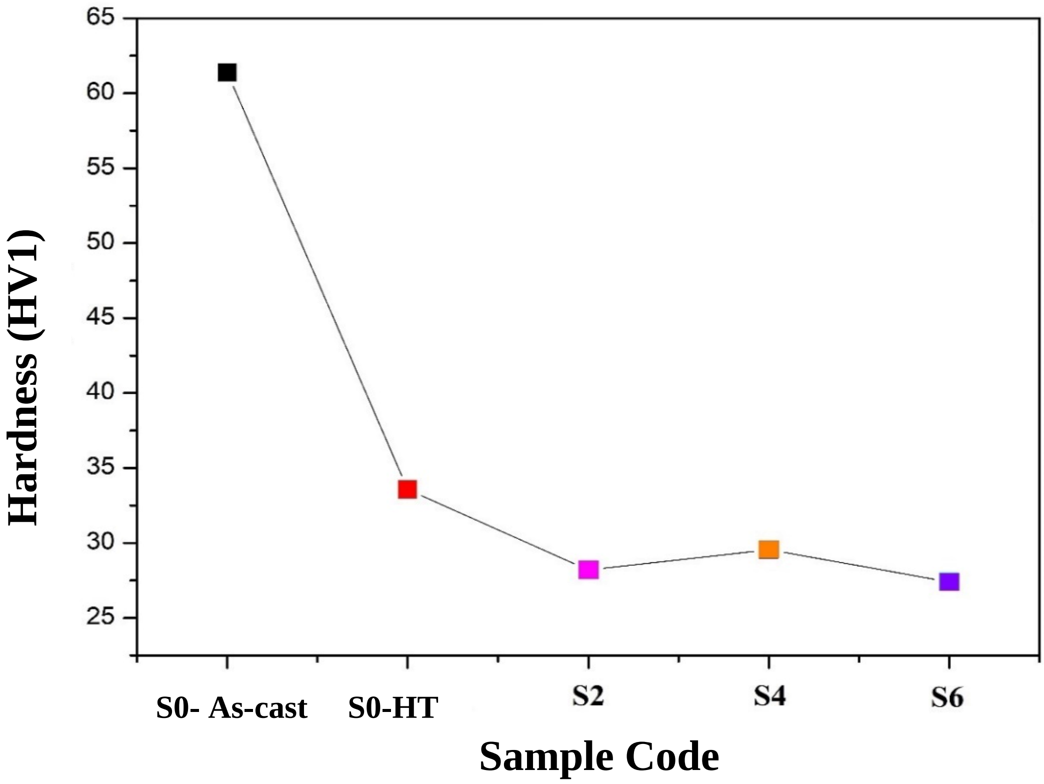

Figure 4. Average hardness values of the standard alloy in the as-cast condition (S0-As cast), the homogenized standard alloy (S0-HT), and Sm-added homogenized alloys (0.2 wt.% – S2, 0.4 wt.% – S4, 0.6 wt.% – S6).

4. Conclusions

In this study, the effects of samarium (Sm) addition on the microstructural and mechanical properties of Al–Fe–Mn alloys were investigated. Experimental findings revealed that increasing Sm content reduced the eutectic structure, significantly refined the grain size, and promoted a more homogeneous distribution of Fe-based intermetallic phases. The formation of Sm–Fe intermetallic compounds such as Sm_2Fe, Sm_3Fe, and Sm_5Fe was confirmed, and these phases were found to contribute to the increase in hardness values. However, the limited coherency of Sm phases with the aluminum matrix and their relatively coarse particle sizes restricted the extent of hardness improvement compared to other rare earth elements. Overall, Sm addition offers a promising approach to improving the microstructural homogeneity and mechanical performance of Al–Fe–Mn alloys; nevertheless, optimization of phase–matrix interactions is required to achieve higher efficiency in industrial applications.

References

[1] J. Grasserbauer, Influence of Fe and Mn on the Microstructure Formation in 5xxx Alloys. Materials, **14**(12), 3204 (2021).

[2] A. Medvedev, Intermetallic Phase Evolution in Al–Fe Alloys. Metals, **11**(5), 815 (2021).

[3] M. Vončina, Microstructure Evolution of EN AW 8006. Metals, **10**(3), 419 (2020).

[4] P. Moldovan, Characterization of AA8006 Alloy Foils. ResearchGate, (2020).

[5] J. Wang, Effect of Cooling Rate on the Microstructure and Thermal Expansion Properties of Al–Mn–Fe Alloy. Reviews on Advanced Materials Science, **37**(1), 31–42 (2022).

[6] Y. Huang, Micro-Alloying with Samarium to Enhance the Thermal Conductivity and Mechanical Properties of Al–5Ni Cast Alloys. Crystals, **15**(7), 609 (2025).

[7] G. Aravindh, Influence of Samarium (Sm) Addition on Mechanical and Tribological Performance of the Al–Mg Alloy AA5083. International Journal of Metalcasting, **19**(3), 2345–2364 (2024).

[8] S. Liao, The Success of Fabrication of Pure $SmFe_2$ Phase Film with Outstanding Perpendicular Magnetic Anisotropy. Materials, **17**(9), 2027 (2024).

[9] H. Li, Effect of Sm Addition on Microstructure and Mechanical Properties of Al–Si–Cu Alloys. International Journal of Metalcasting, **12**(3), 554–564 (2018).

[10] J. Pázmán, The Effect of Chemical Composition and Production Technology on the Mechanical Properties of EN AW-8006 Alloy. Acta Materialia Transylvanica, **4**(1), 45–50 (2021).

[11] F. Denizli, Investigation of $Al_6(Fe,Mn)$ Intermetallics Formation on AA8006 Aluminum Alloy. Light Metals 2025, Springer, 1077–1083 (2025).

[12] P. Moldovan, Microstructure and Phase Evolution in Al–Fe–Mn Alloys with Trace Additions. Journal of Materials Science, **60**(1), 14160–14170 (2025).

[13] M. Okur, Effect of Rare Earth Elements on Aluminum Alloys: A Review. Journal of Materials Engineering, **41**(2), 241–246 (2023).